

# Effects of Dynamical Coupling on Biped-walking Behavior

○ Keli Shen(Okayama University) Xiang Li(Okayama University) Daiji Izawa(Okayama University) Mamoru Minami(Okayama University)

## 1. Introduction

In many researches, ZMP control is considered as an effective method to realize the stable walking by keeping the calculated point within the convex hull of supporting area [1]. However, when the calculated point is on the tip of supporting foot, ZMP cannot work effectively, which makes the humanoid tend to fall down. Besides, ZMP control makes the humanoid robots' waist lower and look like monkey while walking. These are drawbacks of ZMP control method. In previous research of our group on VLA in [2], the incomplete model of humanoid was applied in which head, arms and torso were neglected. Thus, there are some drawbacks, i.e., the model was too simple to consider the effect of dynamical coupling of arm and upper body. However, the new model has been optimized concerning the above problem, and the discussion of slipping and effectiveness of the model have been proved in [3].

Visual-lifting Approach(VLA) based on visual servoing has been proposed which can realize the natural walking with slippage including toe-off state. Real-time position and orientation tracking method to observe a 3D object has been proposed as visual pose estimation [4], which is further applied to measure the robot's head relative pose. And some of added feedforward inputs are used to keep the leg joints rotating for walking and another is used to swing the waist, which further swings the arms by dynamical coupling. The simulation result indicates that visual feedback control and feedforward inputs are useful to realize the biped-walking more like human's dynamics includes toe-off, slipping and bumping. What's more important in this paper is that simulation results prove the effects of dynamical coupling on the biped-walking behavior.

## 2. Dynamical Humanoid Walking Model

The biped-walking robot in Fig. 1 is discussed in this paper, Table 1 shows length  $l_i$  [m], mass  $m_i$  [kg] of links and coefficient of joints' viscous friction  $d_i$  [N·m·s/rad], which are determined by [5]. This model is simulated as a serial-link manipulator having branches and represents rigid whole-body such as feet including toe, torso, arms and so on and is up to 17 degree-of-freedom. Though motion of legs is limited in sagittal plane, it generates many walking gaits since the robot has flat-sole feet and kicking torque. In this paper, the foot named as link-1 is defined as "supporting-foot" and the other foot named as link-7 is defined as "free foot" ("contacting-foot" when the floating foot contacts with ground) according to gaits. When the contacting-foot stops slipping which indicates that static

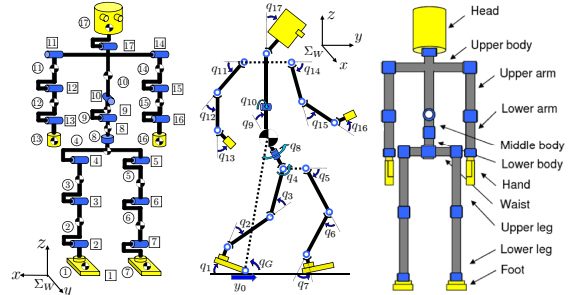


Fig.1 Definition of biped-walking model, ①~⑰ represents link number, ①~⑰ is joint number,  $q_1 \sim q_{17}$  is joint angles.

Table.1 Physical parameters

Link	$l_i$ [m]	$m_i$ [kg]	$d_i$ [Nms/rad]
Head	0.24	4.5	0.5
Upper body	0.41	21.5	10.0
Middle body	0.1	2.0	10.0
Lower body	0.1	2.0	10.0
Upper arm	0.31	2.3	0.03
Lower arm	0.24	1.4	1.0
Hand	0.18	0.4	2.0
Waist	0.27	2.0	10.0
Upper leg	0.38	7.3	10.0
Lower leg	0.40	3.4	10.0
Foot	0.07	1.3	10.0
Total weight [kg]	—	64.2	—
Total high [m]	1.7	—	—

friction force is exerted to the foot, the contacting-foot switches to supporting-foot and the previous supporting-foot is transferred into free foot if it was isolated from floor.

## 3. Dynamical Calculations Based on NE Method

### 3.1 Forward Kinematic Calculations

The equation of motion is derived by following NE formulation [6]. So the structure of the supporting-foot must to be considered with two situations. When the supporting-foot is constituted by rotating joint, the relations of positions made by rotation must be firstly calculated followed by velocities and accelerations between

links as forward kinematics procedures from bottom link to top link. Then if the supporting-foot is slipping, it should be described as a prismatic joint, which is used for the modeling of slippage of foot.

The velocity and acceleration of 4-th link are transmitted to 5-th and 8-th link and ones of 10th link transmit to 11th, 14th and 17th link directly because of ramification mechanisms as shown in Fig.1. For more details about forward kinematic calculation, please read the previous paper [6].

### 3.2 Backward Inverse Dynamical Calculations

After the above forward kinematic calculation has been done, contrarily inverse dynamical calculation from top to base link are shown as follow. Newton equation and Euler equation of  $i$ -th link are represented by Eqs. (1), (2) when  ${}^i\mathbf{I}_i$  is defined as inertia tensor of  $i$ -th link. Here,  ${}^i\mathbf{f}_i$  and  ${}^i\mathbf{n}_i$  in  $\Sigma_i$  show the force and moment exerted on  $i$ -th link from  $(i + 1)$ -th link based on the coordinates  $\Sigma_i$ .

$${}^i\mathbf{f}_i = {}^i\mathbf{R}_{i+1}{}^{i+1}\mathbf{f}_{i+1} + m_i{}^i\ddot{\mathbf{s}}_i \quad (1)$$

$${}^i\mathbf{n}_i = {}^i\mathbf{R}_{i+1}{}^{i+1}\mathbf{f}_{i+1} + {}^i\mathbf{I}_i{}^i\dot{\boldsymbol{\omega}}_i + {}^i\boldsymbol{\omega}_i \times ({}^i\mathbf{I}_i{}^i\boldsymbol{\omega}_i) + {}^i\hat{\mathbf{s}}_i \times (m_i{}^i\ddot{\mathbf{s}}_i) + {}^i\hat{\mathbf{p}}_{i+1} \times ({}^i\mathbf{R}_{i+1}{}^{i+1}\mathbf{f}_{i+1}) \quad (2)$$

On the other hand, since force and torque of 5-th and 8-th links are exerted on 4-th link, effects onto 4-th link is described as:

$${}^4\mathbf{f}_4 = {}^4\mathbf{R}_5{}^5\mathbf{f}_5 + {}^4\mathbf{R}_8{}^8\mathbf{f}_8 + m_4{}^4\ddot{\mathbf{s}}_4, \quad (3)$$

$${}^4\mathbf{n}_4 = {}^4\mathbf{R}_5{}^5\mathbf{n}_5 + {}^4\mathbf{R}_8{}^8\mathbf{n}_8 + {}^4\mathbf{I}_4{}^4\dot{\boldsymbol{\omega}}_4 + {}^4\boldsymbol{\omega}_4 \times ({}^4\mathbf{I}_4{}^4\boldsymbol{\omega}_4) + {}^4\hat{\mathbf{s}}_4 \times (m_4{}^4\ddot{\mathbf{s}}_4) + {}^4\hat{\mathbf{p}}_5 \times ({}^4\mathbf{R}_5{}^5\mathbf{f}_5) + {}^4\hat{\mathbf{p}}_8 \times ({}^4\mathbf{R}_8{}^8\mathbf{f}_8). \quad (4)$$

Similarly, force and torque of 11-th, 14-th and 17-th links transmit to 10-th link directly.

Finally, equation of motion with one foot standing can be derived as:

$$\mathbf{M}(\mathbf{q})\ddot{\mathbf{q}} + \mathbf{h}(\mathbf{q}, \dot{\mathbf{q}}) + \mathbf{g}(\mathbf{q}) + \mathbf{D}\dot{\mathbf{q}} = \boldsymbol{\tau}, \quad (5)$$

For more details about backward inverse dynamical calculations, please read the previous paper [6].

## 4. Biped Walking Control Method

### 4.1 Visual Lifting Approach

This section proposes a visual-lifting feedback to improve the stability of biped standing/walking as shown in Fig. 2. We apply a model-based matching method to measure the posture of a static target object described by  $\boldsymbol{\psi}(t)$  representing the robot's head based on  $\Sigma_H$ . The relatively desired posture of  $\Sigma_R$  (coordinate of reference target object) and  $\Sigma_H$  is predefined by Homogeneous Transformation as  ${}^H\mathbf{T}_R$ . The difference of the desired head posture  $\Sigma_{H_d}$  and the current posture  $\Sigma_H$  is defined as  ${}^H\mathbf{T}_{H_d}$ , it can be described by:

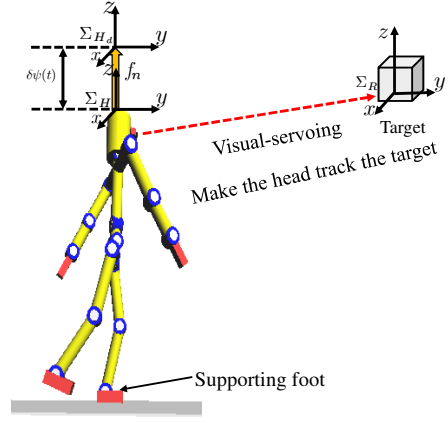


Fig.2 Concept of Visual Lifting Approach.

$${}^H\mathbf{T}_{H_d}(\boldsymbol{\psi}_d(t), \boldsymbol{\psi}(t)) = {}^H\mathbf{T}_R(\boldsymbol{\psi}(t)) \cdot {}^{H_d}\mathbf{T}_R^{-1}(\boldsymbol{\psi}_d(t)), \quad (6)$$

where  ${}^H\mathbf{T}_R$  is calculated by  $\boldsymbol{\psi}(t)$ .  $\boldsymbol{\psi}(t)$  can be measured by on-line visual posture evaluation proposed by [4]. However, we assume that this parameter is given directly. Here, the force is considered to be directly proportional to  $\delta\boldsymbol{\psi}(t)$ , which is exerted on the head to minimize  $\delta\boldsymbol{\psi}(t) (= \boldsymbol{\psi}_d(t) - \boldsymbol{\psi}(t))$  calculated from  ${}^H\mathbf{T}_{H_d}$ . The deviation of the robot's head posture is caused by gravity force and the influence of walking dynamics. The joint torque  $\boldsymbol{\tau}_h(t)$  lifting the robot's head is donated:

$$\boldsymbol{\tau}_h(t) = \mathbf{J}_h(\mathbf{q})^T \mathbf{K}_p \delta\boldsymbol{\psi}(t), \quad (7)$$

where  $\mathbf{J}_h(\mathbf{q})$  in Fig. 2 is Jacobian matrix of the head posture against joint angles from supporting foot to head including  $q_1, q_2, q_3, q_4, q_8, q_9, q_{10}, q_{17}$ , and  $\mathbf{K}_p$  is proportional gain like impedance control. We apply this input to stop falling down caused by gravity or dangerous slipping gaits happened unpredictably during walking progress. We stress that the input torque for non-holonomic joint such as joint-1,  $\tau_{h_1}$  in  $\boldsymbol{\tau}_h(t)$  in Eq. (7) is zero for its free joint.  $\delta\boldsymbol{\psi}(t)$  can show the deviation of the humanoid's position and orientation, however, only position is discussed in this study.

### 4.2 Feedforward Inputs

Besides  $\boldsymbol{\tau}_h(t)$ , in order to make the floating-foot and supporting-foot step forward, added input torques  $\boldsymbol{\tau}_t(t) = [0, \tau_{t2}, \tau_{t3}, 0, \tau_{t5}, \tau_{t6}, \tau_{t7}, 0, \dots, 0]^T$  are used. And another kind of input torques  $\boldsymbol{\tau}_w(t) = [0, \dots, 0, \tau_{w8}, 0, \dots, 0]^T$  is used to swing the roll angle of the waist (joint-8), which further realizes the arm swinging motion through dynamical coupling. Here,  $\boldsymbol{\tau}_t(t)$  and  $\boldsymbol{\tau}_w(t)$  are seen as feed-forward input torques. Here,  $t_2$  means the time that supporting-foot and contacting-foot are switched. The elements  $\boldsymbol{\tau}_t(t)$  and  $\boldsymbol{\tau}_{w8}(t)$  are shown below:

$$\tau_{t5} = \begin{cases} 20\cos(2\pi(t - t_2)/1.45), & (t < 1.0[s]) \\ 15\cos(2\pi(t - t_2)/1.85), & (t \geq 1.0[s]), \end{cases} \quad (8)$$

$$\tau_{w8} = \begin{cases} D\sin 2\pi(t - t_2)/1.85, & (\text{right foot supporting}) \\ -D\sin 2\pi(t - t_2)/1.85, & (\text{left foot supporting}). \end{cases} \quad (9)$$

When time  $t < 1.5[s]$ ,  $\tau_{t2}, \tau_{t3}, \tau_{t6}, \tau_{t7}$  are set as feedback inputs.

$$\tau_{t2} = 40(-0.2 - q_2), \quad (10)$$

$$\tau_{t3} = 50(0.3 - q_3), \quad (11)$$

$$\tau_{t6} = 100(-0.4 - q_6). \quad (12)$$

$$\tau_{t7} = \begin{cases} 60(0.6 - q_7), & (\text{the first step}) \\ 20(0.35 - q_7), & (\text{others}). \end{cases} \quad (13)$$

When time  $t > 1.5[s]$ ,  $\tau_{t2}, \tau_{t3}, \tau_{t6}, \tau_{t7}$  are set as feed-forward inputs.

$$\tau_{t2} = 10\sin(2\pi(t - t_2)), \quad (14)$$

$$\tau_{t3} = -10 + 10\sin(2\pi(t - t_2)), \quad (15)$$

$$\tau_{t6} = -20 + 20\sin(\pi(t - t_2)). \quad (16)$$

$$\tau_{t7} = \begin{cases} 60, & (\text{floating and } q_7 \leq 0.6[\text{rad}]) \\ -40, & (\text{pointcontacting and } q_7 \geq 0.35[\text{rad}]) \\ 0, & (\text{in other cases}). \end{cases} \quad (17)$$

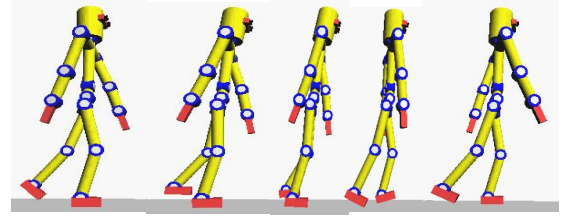
Combining three kinds of torques in Eqs. (6)~(17), the controller for walking is derived,

$$\tau(t) = \tau_h(t) + \tau_t(t) + \tau_w(t). \quad (18)$$

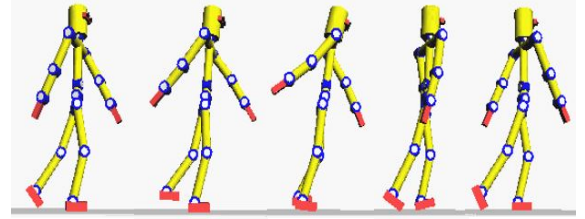
## 5. Effects Analyses of Biped Behavior Based on Dynamical Coupling

In this section,  $D$  in Eq. (9) is set as two different values:  $D = 25$  [Nm] and  $D = 50$  [Nm]. In Eq. (9),  $\tau_{w8}(t)$  is given the opposite value according to which foot is supporting foot, which swings the waist, further realizing the swinging of two arms with the opposite directions.

Figure 4 shows the relation of angle and angular velocity of waist joint. The point (0,0) is the initial state of wait. The red cycle shows the change ranges of angle and angular velocity when  $D$  is set as 25 [Nm], In this case,  $\delta q_8 = 0.48[\text{rad}]$ ,  $\delta \dot{q}_8 = 2.04[\text{rad/s}]$ . When  $D$  is set as 50 [Nm],  $\delta q_8 = 0.96[\text{rad}]$ ,  $\delta \dot{q}_8 = 4.20[\text{rad/s}]$ . According to two group data, when the maximum of  $\tau_{w8}(t)$  changes from 25 [Nm] to 50 [Nm],  $\delta q_8$  and  $\delta \dot{q}_8$  also change about twice correspondingly, which obeys the principle of conservation of energy and Newton's second law of motion.



(a) Screen shot of biped walking when  $D=25$  [Nm]



(b) Screen shot of biped walking when  $D=50$  [Nm]

Fig.3 Screen shots of biped walking after entering stable walking phrase.

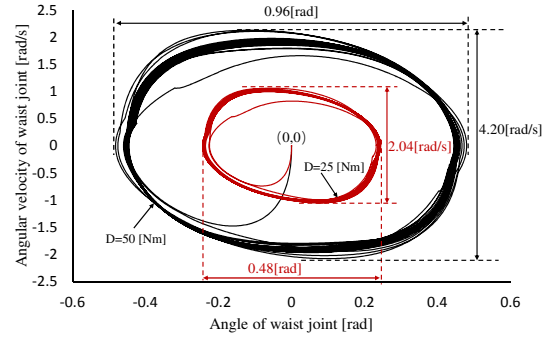


Fig.4 Relation of angle and angular velocity of waist joint.

Figures 5 and 6 show the relation of angle and angular velocity of right shoulder joint and left shoulder joint after 11-th step of walking representatively. From Fig. 5, when  $D$  is set as 25 [Nm],  $\delta q_8 = 0.72[\text{rad}]$ ,  $\delta \dot{q}_8 = 2.87[\text{rad/s}]$ . And when  $D$  is set as 50 [Nm],  $\delta q_8 = 1.62[\text{rad}]$ ,  $\delta \dot{q}_8 = 6.65[\text{rad/s}]$ . Similarly, from Fig. 6, when  $D$  is set as 25 [Nm],  $\delta q_8 = 0.70[\text{rad}]$ ,  $\delta \dot{q}_8 = 2.90[\text{rad/s}]$ . And when  $D$  is set as 50 [Nm],  $\delta q_8 = 1.62[\text{rad}]$ ,  $\delta \dot{q}_8 = 6.34[\text{rad/s}]$ . According to the biped walking control method in last section, there are no inputs in the joints of two arms. Therefore, added waist joint input  $\tau_{w8}(t)$  has an effect on swinging two arms via the dynamical coupling, also indicating about twice relation of angle and angular velocity. Fig. 3 (a) and (b) show the appearance of walking after entering the stable phase correspondingly.

Besides, Fig. 7 shows steplength of walking when  $D = 25$  is bigger than that when  $D = 50$ .

## 6. Conclusion

In this paper, NE method is introduced to explain the calculation of motion parameters and the relation of joint force. Visual Lifting Approach and feedforward inputs can

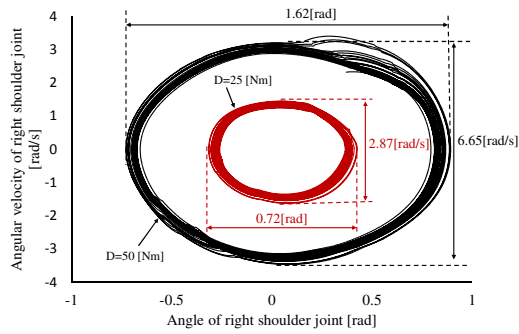


Fig.5 Relation of angle and angular velocity of right shoulder joint.

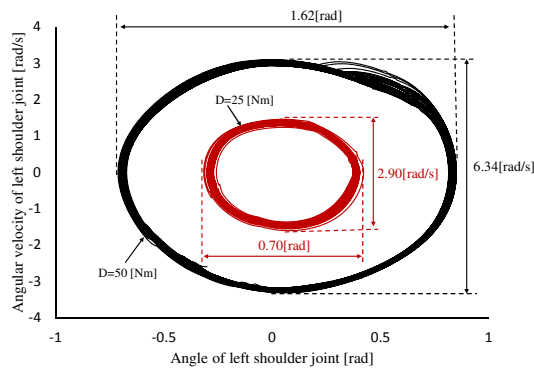


Fig.6 Relation of angle and angular velocity of left shoulder joint.

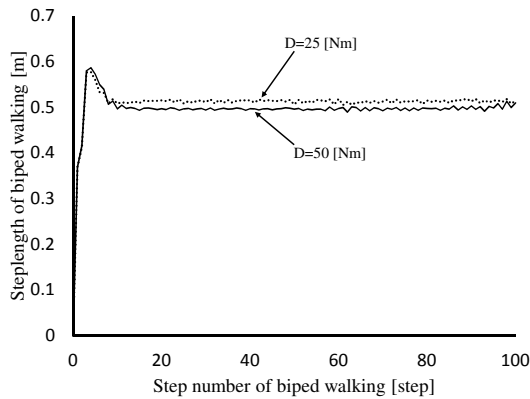


Fig.7 Steplength of biped walking during 100 steps.

make humanoid keep standing and walking. And more importantly, effects of dynamical coupling are verified and analyzed. Waist joint input  $\tau_{ws}(t)$  has influence on walking behavior and swinging the arms. In our future work, we will adjust waist joint input to improve the walking stability and flexibility.

### References

[1] M. Vukobratovic, A. Frank and D. Juricic: On the Stability of Biped Locomotion, IEEE Transactions on Biomedical Engineering, Vol.17, No.1 (1970)

[2] Wei Song, Mamoru Minami and Yanan Zhang: A Visual Lifting Approach for Dynamic Bipedal Walking, International Journal of Advanced Robotic Systems, Vol.9, pp.1-8, 2012.

[3] Xiang Li, Hiroki Imanishi, mamoru Minami, Takayuki Matsuno, Akira Yanou: Dynamical Model of Walking Transition Considering Nonlinear Friction with Floor, Journal of Advanced Computational Intelligence and Intelligent Informatics, Vol.20 No.6, 2016.

[4] F. Yu, W. Song and M. Minami: Visual Servoing with Quick Eye-Vergence to Enhance Trackability and Stability, Proceedings of IEEE/RSJ International Conference on Intelligent Robots and Systems, pp.6228-6233, 2010.

[5] M. Kouchi, M. Mochimaru, H. Iwasawa and S. Mitani: Anthropometric database for Japanese Population 1997-98, Japanese Industrial Standards Center (AIST, MITI), 2000.

[6] T. Maeba, M. Minami, A. Yanou and J. Nishiguchi, "Dynamical Analyses of Humanoid's Walking by Visual Lifting Stabilization Based on Event-driven State Transition," 2012 IEEE/ASME Int. Conf. on Advanced Intelligent Mechatronics Proc., pp.7-14, 2012.